Article

Heterolytic Cleavage of Dihydrogen Promoted by Sulfido-Bridged Tungsten–Ruthenium Dinuclear Complexes

Yasuhiro Ohki, Nobuo Matsuura, Tadashi Marumoto, Hiroyuki Kawaguchi, and Kazuyuki Tatsumi

J. Am. Chem. Soc., **2003**, 125 (26), 7978-7988• DOI: 10.1021/ja029941x • Publication Date (Web): 07 June 2003

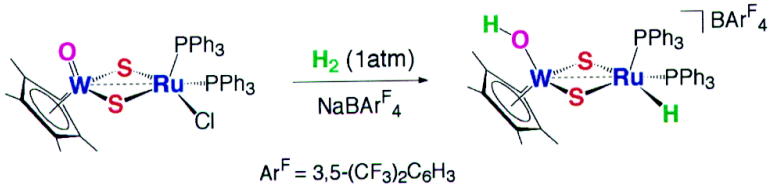

J|A|C|S
ARTICLES
Published on Web 06/07/2003

Heterolytic Cleavage of Dihydrogen Promoted by Sulfido-Bridged Tungsten−Ruthenium Dinuclear Complexes

Yasuhiro Ohki, Nobuo Matsuura, Tadashi Marumoto, Hiroyuki Kawaguchi,† and Kazuyuki Tatsumi*

Contribution from the Department of Chemistry, Graduate School of Science and Research Center for Materials Science, Nagoya University, Furo-cho, Chikusa-ku, Nagoya 464-8602, Japan

Received December 27, 2002; E-mail: i45100a@nucc.cc.nagoya-u.ac.jp

Abstract: A series of sulfido-bridged tungsten−ruthenium dinuclear complexes Cp*W(μ-S)$_3$RuX(PPh$_3$)$_2$ (**4a**; X = Cl, **4b**; X = H), Cp*W(O)(μ-S)$_2$RuX(PPh$_3$)$_2$ (**5a**; X = Cl, **5b**; X = H), and Cp*W(NPh)(μ-S)$_2$RuX(PPh$_3$)$_2$ (**6a**; X = Cl, **6b**; X = H) have been synthesized by the reactions of (PPh$_4$)[Cp*W(S)$_3$] (**1**), (PPh$_4$)[Cp*W(O)(S)$_2$] (**2**), and (PPh$_4$)[Cp*W(NPh)(S)$_2$] (**3**), with RuClX(PPh$_3$)$_3$ (X = Cl, H). The heterolytic cleavage of H$_2$ was found to proceed at room temperature upon treating **5a** and **6a** with NaBAr$^F_4$ (Ar^F = 3, 5-C$_6$H$_3$(CF$_3$)$_2$) under atmospheric pressure of H$_2$, which gave rise to [Cp*W(OH)(μ-S)$_2$RuH(PPh$_3$)$_2$](BAr$^F_4$) (**7a**) and [Cp*W(NHPh)(μ-S)$_2$RuH(PPh$_3$)$_2$](BAr$^F_4$) (**8**), respectively. When Cp*W(O)(μ-S)$_2$Ru(PPh$_3$)$_2$H (**5b**) was treated with a Brϕnstead acid, [H(OEt$_2$)$_2$](BAr$^F_4$) or HOTf, protonation occurred exclusively at the terminal oxide to give [Cp*W(OH)(μ-S)$_2$RuH(PPh$_3$)$_2$](X) (**7a**; X = BAr$^F_4$, **7b**; X = OTf), while the hydride remained intact. The analogous reaction of Cp*W(μ-S)$_3$Ru(PPh$_3$)$_2$H (**4b**) led to immediate evolution of H$_2$. Selective deprotonation of the hydroxyl group of **7a** or **7b** was induced by NEt$_3$ and **4b**, generating Cp*W(O)(μ-S)$_2$Ru(PPh$_3$)$_2$H (**5b**). Evolution of H$_2$ was also observed for the reactions of **7a** or **7b** with CH$_3$CN to give [Cp*W(O)(μ-S)$_2$Ru(CH$_3$CN)(PPh$_3$)$_2$](X) (**11a**; X = BAr$^F_4$, **11b**; X = OTf). We examined the H/D exchange reactions of **4b**, **5b**, and **7a** with D$_2$ and CH$_3$OD, and found that facile H/D scrambling over the W−OH and Ru−H sites occurred for **7a**. Based on these experimental results, the mechanism of the heterolytic H$_2$ activation and the reverse H$_2$ evolution reactions are discussed.

Introduction

Activation of molecular hydrogen is one of the fundamentally important reactions in organometallic chemistry,[1] and homolytic cleavage of the H−H bond to give two hydrides can be achieved via oxidative addition reactions on electron-rich transition metals. However, the splitting of dihydrogen into a hydride and a proton is less common. Heterolytic H−H cleavage has been found to occur on mononuclear complexes in two ways; (1) deprotonation of η^2-coordinated H$_2$ with external or internal bases,[2−4] and (2) addition of H$_2$ to M−E bonds (E = N, O, S) to generate M−H and E−H bonds.[5] For instance, the acidic dihydrogen in [Cp*Re(CO)(NO)(H$_2$)]$^+$ can be deprotonated by diethyl ether,[3b] and the ruthenium complex with a tethered N-donor group, [(η^5:η^1-C$_5$H$_4$(CH$_2$)$_3$NMe$_2$)Ru(dppm)](BF$_4$), activates H$_2$ (60 atm) to afford [(η^5:η^1-C$_5$H$_4$(CH$_2$)$_3$NHMe$_2$)RuH(dppm)](BF$_4$), presumably via coordination of H$_2$ at Ru and the subsequent intramolecular deprotonation.[4c] Dihydrogen is reversibly added to the Ti=S bond of a titanocene sulfido complex Cp*$_2$TiS(py), generating Cp*$_2$Ti(H)(SH).[5b,c] Some S-bridged dinuclear complexes are also capable of promoting heterolytic H$_2$ cleavage.[6] An early example is a cationic Rh$_2$ complex [{Rh(triphos)}$_2$(μ-S)$_2$]$^{2+}$ (triphos = tris(diphenylphosphinomethyl)ethane), which is converted to [{RhH(triphos)}$_2$(μ-SH)$_2$]$^{2+}$ by

† Present address: Coordination Chemistry Laboratory, Institute for Molecular Science, Myodaiji, Okazaki, 444-8595, Japan.

(1) (a) Kristjánsdóttir, S. S.; Norton, J. R. In *Transition Metal Hydrides: Recent Advances in Theory and Experiment*; Dedieu, A., Ed.; VCH: New York, 1992. (b) Jessop, P. G.; Morris, R. H. *Coord. Chem. Rev.* **1992**, *121*, 155. (c) Kubas, G. J. In *Metal Dihydrogen and σ-Bond Complexes*; Kluwer Academic/Plenum Publishers: New York, 2001. (d) *Recent Advances in Hydride Chemistry*; Peruzzini, M., Poli, R., Eds.; Elsevier: Amsterdam, 2001.

(2) (a) Kristjánsdóttir, S. S.; Moody, A. E.; Weberg, R. T.; Norton, J. R. *Organometallics* **1988**, *7*, 1983. (b) Weberg, R. T.; Norton, J. R. *J. Am. Chem. Soc.* **1990**, *112*, 1105. (c) Kristjánsdóttir, S. S.; Loendorf, A. J.; Norton, J. R. *Inorg. Chem.* **1991**, *30*, 4470. (d) Morris, R. H. *Inorg. Chem.* **1992**, *31*, 1471. (e) Angelici, R. J. *Acc. Chem. Res.* **1995**, *28*, 51. (f) Jia, G. C.; Lau, C. P. *Coord. Chem. Rev.* **1999**, *192*, 83. (g) Abdur-Rashid, K.; Fong, T. P.; Greaves, Bronwyn, Gusev, D. G.; Hinman, J. G.; Landau, S. E.; Lough, A. J.; Morris, R. H. *J. Am. Chem. Soc.* **2000**, *122*, 9155.

(3) (a) Chinn, M. S.; Heinekey, D. M. *J. Am. Chem. Soc.* **1987**, *109*, 5865. (b) Chinn, M.; Heinekey, D. M.; Payne, N. G.; Sofield, C. D. *Organometallics* **1989**, *8*, 1824. (c) Lopez, L. L.; Bernatis, P.; Birnbaum, J.; Haltiwanger, R. C.; DuBois, M. R. *Organometallics*, **1992**, *11*, 2424. (d) Bianchini, C.; Marchi, A.; Rossi, R.; Vacca, A. *Organometallics* **1995**, *14*, 3203. (e) Smith, K. T.; Tilset, M.; Kuhlman, R.; Caulton, K. G. *J. Am. Chem. Soc.* **1995**, *117*, 9473. (f) Ayllon, J. A.; Gervaux, C.; Sabo-Etienne, S.; Chaudret, B. *Organometallics* **1997**, *16*, 2000. (g) Jia, G.; Lee, H. M.; Williams, I. D.; Lau, C. P.; Chen, Y.-Z. *Organometallics* **1997**, *16*, 3941. (h) Belkova, N. V.; Bakhmutova, E. V.; Shubina, E. S.; Bianchini, C.; Peruzzini, M.; Bakhmutov, V. I.; Epstein, L. M. *Eur. J. Inorg. Chem.* **2000**, 2163.

(4) (a) Lough, A. J.; Park, S.; Ramachandra, R.; Morris, R. H. *J. Am. Chem. Soc.* **1994**, *116*, 8356. (b) Lee, Jr. J. C.; Peris, E.; Rheingold, A. L.; Crabtree, R. H. *J. Am. Chem. Soc.* **1994**, *116*, 11 014. (c) Chu, H. S.; Lau, C. P.; Wong, K. Y.; Wong, W. T. *Organometallics* **1998**, *17*, 2768. (d) Ogo, S.; Makihara, N.; Kaneko, Y.; Watanabe, Y. *Organometallics* **2001**, *20*, 497.

(5) (a) Schlaf, M.; Lough, A. J.; Morris, R. H. *Organometallics* **1996**, *15*, 4423. (b) Sweeney, Z. K.; Polse, J. L.; Andersen, R. A.; Bergman, R. G.; Kubinec, M. G. *J. Am. Chem. Soc.* **1997**, *119*, 4543. (c) Sweeney, Z. K.; Polse, J. L.; Bergman, R. G.; Andersen, R. A. *Organometallics*, **1999**, *18*, 5502. (d) Sellman, D.; Rackelmann, G. H.; Heinemann, F. W. *Chem. Eur. J.* **1997**, *3*, 2071.

10.1021/ja029941x CCC: $25.00

the reaction with H_2.[6b] Later, a neutral Ir_2 complex $[Ir(PPh_3)_2]_2(\mu\text{-}S)_2$ was shown to react with two equiv of H_2, via homolytic and subsequent heterolytic pathways, and to eventually produce $[IrH(PPh_3)_2]_2(\mu\text{-}H)(\mu\text{-}S)(\mu\text{-}SH)$.[6c] More recently, the reaction of $[Cp_2W(\mu\text{-}S)_2Ir(PPh_3)_2]^+$ with H_2 (10 atm) was reported to give three products, one of which was characterized as $[Cp_2W(\mu\text{-}SH)_2Ir(H)_2(PPh_3)_2]^+$ based on the ^{31}P NMR spectra.[6d]

The heterolytic cleavage of H_2 has also been regarded as a key step in the metalloenzymatic reactions of hydrogenases, the active sites of which consist of the sulfur-bridged Fe/Fe and Fe/Ni dinuclear centers.[7] To provide a clue to understand the reversible processes of biological H_2 activation, it is desirable to propose model reactions of the heterolytic H_2 activation on dinuclear metal centers,[8] in addition to build the structural models of the active sites.[9] Soluble transition metal sulfido clusters are attractive candidates for the investigation of the mechanism of H_2 activation. However, the construction of appropriate sulfur-bridged dinuclear systems which are reactive toward molecular hydrogen remains difficult, since dinucleation reactions often give rise to less reactive products. One of the effective ways to link two different metal centers by sulfur atoms is to use transition metal sulfido complexes as precursors. We have previously synthesized a series of tungsten thio complexes such as $(PPh_4)[Cp^*W(S)_3]$ (**1**), $(PPh_4)[Cp^*W(O)(S)_2]$ (**2**), and $(PPh_4)[Cp^*W(O)(S)(Se)]$,[10] and have demonstrated that they were convenient entries into the construction of various heterometallic sulfido clusters with Fe, Cu, Pd, Ag, and Au.[11]

Scheme 1

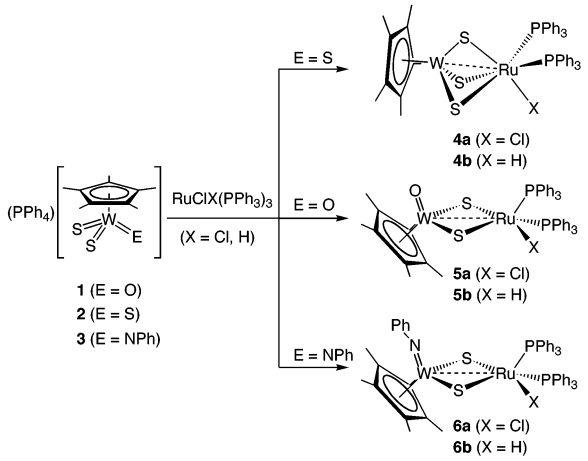

Aiming to obtain reactive dinuclear sulfido complexes, the half-sandwich thio complexes of tungsten were combined with appropriate ruthenium complexes. Having both electron-rich and electron-deficient metal centers linked by sulfur atoms within a molecule, the W−Ru complexes might be anticipated to promote a new type of H_2 activation. Thus, $(PPh_4)[Cp^*W(S)_3]$ (**1**), $(PPh_4)[Cp^*W(O)(S)_2]$ (**2**), and $(PPh_4)[Cp^*W(NPh)(S)_2]$ (**3**) were used as building blocks and reacted with $RuCl_2(PPh_3)_3$ and $RuCl(H)(PPh_3)_3$. Here we report a series of S-bridged W−Ru dinuclear complexes obtained therefrom, and a thorough investigation of their reactivity toward H_2 and protons. To assess the mechanism of H_2 activation by the W−Ru complexes, H/D exchange reactions were also carried out with the hydrogenated products, and their deprotonation and H_2 dissociation reactions were examined.

Results and Discussion

Synthesis of S−Bridged W−Ru Complexes. A series of W−Ru dinuclear complexes were synthesized in high yield from the reactions of half-sandwich dithio- and trithio-complexes of W(VI) with phosphine/chloride complexes of Ru(II). The reactions of the tungsten trithio complex $(PPh_4)[Cp^*W(S)_3]$ (**1**) with 1 equiv of $RuCl_2(PPh_3)_3$ and $RuCl(H)(PPh_3)_3$[12] in CH_3CN at room temperature yielded the W−Ru complexes with three bridging sulfides, $Cp^*W(\mu\text{-}S)_3RuX(PPh_3)_2$ (**4a**; X = Cl, **4b**; X = H), in 77% and 83% yields, respectively. The crystals obtained from a CH_2Cl_2/hexane solution of **4a** and those from a toluene/hexane solution of **4b** were subjected to X-ray structure analysis. These compounds are moderately sensitive toward oxygen and moisture, and the combustion analysis and the ^1H and $^{31}P\{^1H\}$ NMR spectra are in accord with the formulation. The two phosphine ligands at Ru are equivalent in the $^{31}P\{^1H\}$ NMR spectra for both **4a** and **4b**. In the case of **4b**, a triplet signal at $\delta = -10.30$ in the ^1H NMR spectrum and the IR ν(Ru−H) band at 1930 cm^{-1} suggest the existence of a Ru−H bond. Thus during the reactions of $(PPh_4)[Cp^*W(S)_3]$ (**1**) with $RuCl(X)(PPh_3)_3$ (X = Cl, H), one phosphine ligand is liberated along with the formation of PPh_4Cl, while one chloride ligand or one hydride ligand remains intact at the Ru center.

The reaction of $(PPh_4)[Cp^*W(O)(S)_2]$ (**2**) with $RuClX(PPh_3)_3$ (X = Cl, H) followed by a standard workup afforded the

(6) (a) Laurie, J. C. V.; Duncan, L. D.; Haltiwanger, R. C.; Weberg, R. T.; Rakowski DuBois, M. *J. Am. Chem. Soc.* **1986**, *108*, 6234. (b) Bianchini, C.; Mealli, C.; Meli, A.; Sabat, M. *Inorg. Chem.* **1986**, *25*, 4618. (c) Linck, R. C.; Pafford, R. J.; Rauchfuss, T. B. *J. Am. Chem. Soc.* **2001**, *123*, 8856. (d) Kato, H.; Seino, H.; Mizobe, Y.; Hidai, M. *J. Chem. Soc., Dalton Trans.* **2002**, 1494.

(7) (a) Volbeda, A.; Charon, M.-H.; Piras, C.; Hatchikian, E. C.; Frey, M.; Fontecilla-Camps, J. C. *Nature*, **1995**, *373*, 580. (b) Happe, R. P.; Roseboom, W.; Pierik, A. J.; Albracht, S. P.; Bagley, K. A. *Nature*, **1997**, *385*, 126. (c) Frey, M. *Struct. Bonding* **1998**, *90*, 97. (d) Ogata, H.; Mizoguchi, Y.; Mizuno, N.; Miki, K.; Adachi, S.-I.; Yasuoka, N.; Yagi, T.; Yamauchi, O.; Hirota, S.; Higuchi, Y. *J. Am. Chem. Soc.* **2002**, *124*, 11 628.

(8) (a) Lawrence, J. D.; Li, H.; Rauchfuss, T. B.; Bénard, M.; Rohmer, M.-M. *Angew. Chem., Int. Ed. Engl.* **1999**, *38*, 3178. (b) Gloaguen, F.; Lawrence, J. D.; Rauchfuss, T. B. *J. Am. Chem. Soc.* **2001**, *123*, 9476. (c) Zhao, X.; Georgakaki, I. P.; Miller, M. L.; Yarbrough, J. C.; Darensbourg, M. Y. *J. Am. Chem. Soc.* **2001**, *123*, 9710. (d) Zhao, X.; Georgakaki, I. P.; Miller, M. L.; Mejia-Rodriguez, R.; Chiang, C.-Y.; Darensbourg, M. Y. *Inorg. Chem.* **2002**, *41*, 3917. (e) Pavlov, M.; Siegbahn, P. E. M.; Blomberg, M. R. A.; Crabtree, R. H. *J. Am. Chem. Soc.* **1998**, *120*, 548. (f) Niu, S.; Thomson, L. M.; Hall, M. B. *J. Am. Chem. Soc.* **1999**, *121*, 4000.

(9) (a) Osterloh, F.; Saak, W.; Pohl, S. *J. Chem. Soc., Chem. Commun.* **1997**, 979. (b) Lai, C.-H.; Reibenspies, J. H.; Darensbourg, M. Y. *Angew. Chem., Int. Ed. Engl.* **1996**, *35*, 2390. (c) Steinfeld, G.; Kersting, B. *J. Chem. Soc., Chem. Commun.* **2000**, 205. (d) Smith, M. C.; Longhurst, S.; Barclav, J. E.; Cramer, S. P.; Davies, S. C.; Hughes, D. L.; Gu, W.-W.; Evans, D. J. *J. Chem. Soc., Dalton Trans.* **2001**, 1387. (e) Davies, S. C.; Evans, D. J.; Hughes, D. L.; Longhurst, S.; Sanders, J. R. *J. Chem. Soc., Chem. Commun.* **1999**, 1935. (f) Sellmann, D.; Geipel, F.; Lauderbach, F.; Heinemann, F. W. *Angew. Chem., Int. Ed. Engl.* **2002**, *41*, 632. (g) Musie, G.; Farmer, P. J.; Tuntulani, T.; Reibenspies, J. H.; Darensbourg, M. Y. *Inorg. Chem.* **1996**, *35*, 2176. (h) Liaw, W.-F.; Chiang, C.-Y.; Lee, G. H.; Peng, S.-M.; Lai, C.-H.; Darensbourg, M. Y. *Inorg. Chem.* **2000**, *39*, 480. (i) Schmidt, M.; Contakes, S. M.; Rauchfuss, T. B. *J. Am. Chem. Soc.* **1999**, *121*, 9736. (j) Lyon, E. J.; Georgakaki, I. P.; Reibenspies, J. H.; Darensbourg, M. Y. *Angew. Chem., Int. Ed. Engl.* **1999**, *38*, 3178. (k) Lawrence, J. D.; Li, H.; Rauchfuss, T. B.; Bénard, M.; Rohmer, M.-M. *Angew. Chem., Int. Ed. Engl.* **2001**, *40*, 1768. (l) Razavet, M.; Davies, S. C.; Hughes, D. L.; Pickett, C. J. *J. Chem. Soc., Chem. Commun.* **2001**, 847.

(10) (a) Kawaguchi, H.; Yamada, K.; Lang, J.-P.; Tatsumi, K. *J. Am. Chem. Soc.* **1997**, *119*, 10 346. (b) Kawaguchi, H.; Tatsumi, K. *Angew. Chem., Int. Ed.* **2000**, *40*, 1266.

(11) (a) Lang, J.-P.; Tatsumi, K. *Inorg. Chem.* **1998**, *37*, 160. (b) Lang, J.-P.; Kawaguchi, H.; Ohnishi, S.; Tatsumi, K. *Inorg. Chim. Acta*, **1998**, *283*, 136. (c) Lang, J.-P.; Kawaguchi, H.; Tatsumi, K. *J. Organomet. Chem.* **1998**, *569*, 109. (d) Lang, J.-P.; Tatsumi, K. *Inorg. Chem.* **1999**, *38*, 1364. (e) Lang, J.-P.; Tatsumi, K. *J. Organomet. Chem.* **1999**, *579*, 332. (f) Lang, J.-P.; Kawaguchi, H.; Tatsumi, K. *J. Chem. Soc., Chem. Commun.* **1999**, 2315.

(12) (a) Hallma, P. S.; Stephenson, T. A.; Wilkinson, G. *Inorg. Synth.* **1972**, *12*, 238. (b) Schunn, R. A.; Wonchoba, E. R. *Inorg. Synth.* **1972**, *13*, 131.

Table 1. Selected Bond Distances (Å) and Angles (deg) for Cp*W(μ-S)$_3$RuX(PPh$_3$)$_2$ (X = Cl (**4a**), H (**4b**)) and Cp*W(O)(μ-S)$_2$RuX(PPh$_3$)$_2$ (X = Cl (**5a**), H (**5b**))

4a		**4b**		**5a**		**5b**	
W−Ru	2.6188(2)	W−Ru	2.6106(3)	W−Ru	2.8511(4)	W−Ru	2.8492(4)
W−S1	2.2302(7)	W−S1	2.2226(8)	W−O	1.746(4)	W−O	1.730(4)
W−S2	2.2159(7)	W−S2	2.2253(7)	W−S1	2.261(1)	W−S1	2.264(1)
W−S3	2.2314(7)	W−S3	2.2367(9)	W−S2	2.250(1)	W−S2	2.276(1)
Ru−S1	2.4079(7)	Ru−S1	2.5387(8)	Ru−S1	2.320(1)	Ru−S1	2.329(1)
Ru−S2	2.4981(8)	Ru−S2	2.4719(8)	Ru−S2	2.230(1)	Ru−S2	2.331(1)
Ru−S3	2.5056(7)	Ru−S3	2.4931(8)	Ru−Cl	2.428(1)	Ru−H	1.62(5)
Ru−Cl	2.4192(7)	Ru−H	1.56(3)	W−S1−Ru	76.96(4)	W−S1−Ru	76.67(4)
W−S1−Ru	68.63(2)	W−S1−Ru	66.11(2)	W−S2−Ru	76.98(4)	W−S2−Ru	76.39(3)
W−S2−Ru	67.19(2)	W−S2−Ru	67.29(2)				
W−S3−Ru	66.83(2)	W−S3−Ru	66.75(2)				

analytically pure W−Ru bis(μ-sulfido) complexes Cp*W(O)(μ-S)$_2$RuX(PPh$_3$)$_2$ (**5a**; X = Cl, **5b**; X = H) in 82% and 86% yields, respectively. In these dinuclear complexes, the oxo ligand does not bridge the two metal centers, as suggested by the characteristic ν(W═O) bands at 895 cm^{-1} (**5a**) and 901 cm^{-1} (**5b**) in the IR spectra.[13] The X-ray quality crystals were grown by layering hexane onto a CH_2Cl_2 solution of **5a** or onto a toluene solution of **5b**. Again, one phosphine ligand was removed from Ru during the reactions, and coordination of a chloride or a hydride ligand at Ru was retained. In a similar manner, the W−Ru complexes having a W═NPh moiety, Cp*W(NPh)(μ-S)$_2$RuX(PPh$_3$)$_2$ (**6a**; X = Cl, **6b**; X = H) were synthesized using (PPh$_4$)[Cp*W(NPh)(S)$_2$] (**3**),[12] which were characterized by ^{1}H and ^{31}P{^{1}H} NMR spectra, IR, and by FAB-mass for **6a**. Their NMR spectra resemble those of the corresponding W−Ru complexes having a terminal oxo group, **5a** and **5b**. The IR spectra are featured by the bands at 1336 cm^{-1} (**6a**) and 1346 cm^{-1} (**6b**) which are assignable to the W═NPh stretching vibrations.[14]

There appear two doublets in the ^{31}P{^{1}H} NMR spectra of the chloride complexes, **5a** and **6a,** at room temperature, indicating that the two phosphine ligands are chemically nonequivalent. This observation is consistent with the solid-state structure of **5a** as will be shown below. On the other hand, the ^{31}P{^{1}H} NMR spectra of the hydride congeners, **5b** and **6b**, show a single peak at room temperature. However, the phosphorus signal for **5b** was found to be significantly broadened with lowering the temperature, and to split into two broad peaks at −85 °C. Thus the site exchange of the two phosphine ligands occurs more readily for the hydride complexes.

Structures of the W−Ru Dinuclear Complexes. The X-ray structure analyses were carried out for Cp*W(μ-S)$_3$RuX(PPh$_3$)$_2$ (**4a**; X = Cl, **4b**; X = H) and Cp*W(O)(μ-S)$_2$RuX(PPh$_3$)$_2$ (**5a**; X = Cl, **5b**; X = H), and selected geometrical parameters are summarized in Table 1. Since their molecular structures are very similar to those of **4b** and **5b**, the perspective views of only the latter two hydride complexes are shown in Figure 1. The hydrides were located at reasonable positions in the last Fourier maps, and they are included in the drawings. For **4a** and **4b**, three sulfur atoms bridge the Cp*W unit and Ru, and the slightly distorted octahedral geometry at Ru is completed by coordination of two phosphine ligands and a chloride (or a hydride). In the case of **5a** and **5b**, the two metal centers are linked by two sulfur atoms, and the Ru site assumes a square pyramidal geometry with one phosphine at the apical site. Consequently, the two phosphines are nonequivalent in the solid state, while those of **5b** are fluxional in solution on the ^{31}P{^{1}H} NMR time scale. The WS_2Ru rhomboids are slightly puckered, where the dihedral angles between the WS_2 and RuS_2 planes are 18.5° (**5a**) and 10.5° (**5b**). The apical phosphine coordination for the hydride complex **5b** tilts notably toward the less bulky hydride position. Thus the W−Ru−P1 angle of 120.0° for **5b** is large, compared with the corresponding angle of 100.7° for the

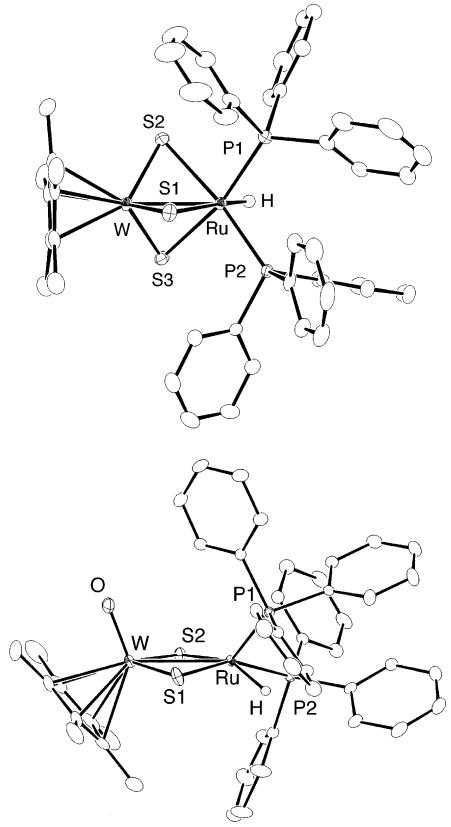

Figure 1. Molecular structures of Cp*W(μ-S)$_3$RuH(PPh$_3$)$_2$ (**4b**) (top) and Cp*W(O)(μ-S)$_2$RuH(PPh$_3$)$_2$ (**5b**) (bottom).

(13) (a) Faller, J. W.; Ma, Y. *Organometallics* **1988**, *7*, 559. (b) Legzdins, P.; Phillips, E. C.; Rettig, S. J.; Sánchez, L.; Trotter, J.; Yee, V. C. *Organometallics* **1988**, *7*, 1877. (c) Faller, J. W.; Ma, Y. *Organometallics* **1989**, *8*, 609. (d) Gorzellik, M.; Bock, H.; Gang, L.; Nuber, B.; Ziegler, M. L. *J. Organomet. Chem.* **1991**, *412*, 95. (e) Rau, M. S.; Kretz, C. M.; Geoffroy, G. L.; Rheingold, A. L. *Organometallics* **1993**, *12*, 3447. (f) Rau, M. S.; Kretz, C. M.; Geoffroy, G. L.; Rheingold, A. L.; Haggerty, B. S. *Organometallics* **1994**, *13*, 1624. (g) Chakraborty, D.; Bhattacharjee, M.; Krätzner, Siefken, R.; Roesky, H. W.; Uson, I.; Schmidt, H.-G. *Organometallics*, **1999**, *18*, 106.

(14) (a) Glassman, T. E.; Vale, M. G.; Schrock, R. R. *Organometallics* **1991**, *10*, 4046. (b) Legzdins, P.; Phillips, E. C.; Rettig, S. J.; Trotter, J.; Veltheer, J. E.; Yee, V. C. *Organometallics* **1992**, *11*, 3104.

Table 2. Selected Bond Distances (Å) and Angles (deg) for [Cp*W(OH)(μ-S)$_2$RuH(PPh$_3$)$_2$](BAr$^F_4$) (**7a**·2C$_4$H$_{10}$O) and [Cp*W(OH)(μ-S)$_2$RuH(PPh$_3$)$_2$](OTf) (**7b**)

7a				**7b**			
W−Ru	2.8124(5)	Ru−H	1.56(6)	W−Ru	2.8306(4)	Ru−H	1.68(8)
W−O1	1.829(4)	O1−O2	2.580(7)	W−O1	1.858(4)	O1−O2	2.66(1)
W−S1	2.248(1)	W−S1−Ru	75.68(4)	W−S1	2.249(1)	W−S1−Ru	76.49(3)
W−S2	2.232(1)	W−S2−Ru	76.84(4)	W−S2	2.233(1)	W−S2−Ru	77.30(4)
Ru−S1	2.335(1)			Ru−S1	2.322(1)		
Ru−S2	2.291(1)			Ru−S2	2.299(1)		

Scheme 2

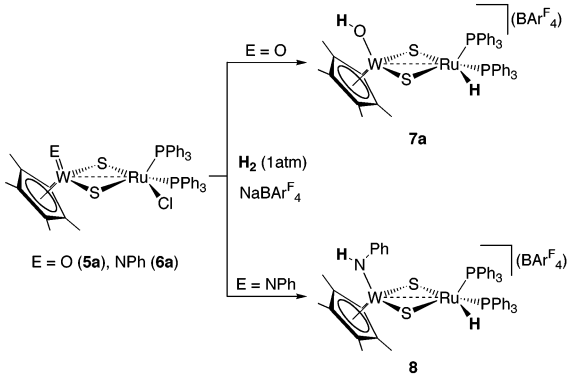

chloride congener **5a**. The W═O bond lengths of 1.746(4) and 1.730(4) Å are as expected for multiple bonding.[14]

The W−S distances of 2.2159(7) − 2.2367(9) for **4a** and **4b** are similar to those of Cp*W(S)(μ-S)$_2$FeCl$_2$ (W-μS; av. 2.25 Å),[15] and fall between the W−S (thiolate) single bond lengths of half-sandwich thiolate complexes of W(VI) (2.33−2.45 Å)[10,16] and the W═S multiple bond lengths of (PPh$_4$)[Cp*W(S)$_3$] (**1**) (av. 2.19 Å).[10a] Thus, there appears to be partial W−S multiple bond character in the W−Ru dinuclear structures, and their oxidation states were assigned to be W(VI) and Ru(II). For **4b**, the Ru−S1 bond which is trans to the hydride ligand is 0.046−0.067 Å longer than the other two Ru−S bonds, which accounts for the strong trans influence of hydride.[17] On the other hand, the Ru−S bonds of **5a** and **5b** are substantially short, while the W−S bonds are elongated, compared with those of the triply bridging structures of **4a** and **4b**. This may have something to do with the different coordination numbers of Ru, and the coordinatively unsaturated Ru centers of **5a** and **5b** could be stabilized by π-interactions with the bridging sulfides. The observed W−Ru distances indicate dative bonding between the electron rich Ru(II) center and the electron deficient W(VI) center, where the triply bridged W−Ru bonds of **4a** and **4b** are much shorter and the W−S−Ru angles are more acute.

Activation of H_2 by the W−Ru Complexes. Considering the coordinative unsaturation of Ru in Cp*W(O)(μ-S)$_2$RuX(PPh$_3$)$_2$ (**5a**; X = Cl, **5b**; X = H), their reactions with H_2 were examined. There was no sign of reaction upon heating a CH_2Cl_2 solution of **5a** or **5b** under 10 atm of H_2. However, when **5a** was treated in CH_2Cl_2 with NaBAr$^F_4$ (Ar^F = 3,5-(CF$_3$)$_2$C$_6$H$_3$)[18] under 1 atm of H_2, we noticed a quick color change of the solution from dark green to purple. The reaction was complete within five minutes at room temperature, and [Cp*W(OH)(μ-S)$_2$RuH(PPh$_3$)$_2$][BAr$^F_4$] (**7a**) was isolated as a purple powder in 84% yield. Thus in this reaction, H_2 splits into the hydridic center attached to Ru and the protic center at the oxo ligand, where the formal oxidation states of the metal atoms are unchanged. The imido analogue of **5a**, Cp*W(NPh)(μ-S)$_2$RuCl(PPh$_3$)$_2$ (**6a**), was also found to activate atmospheric H_2 under the presence of NaBAr$^F_4$, resulting in the formation of [Cp*W(NHPh)(μ-S)$_2$RuH(PPh$_3$)$_2$][BAr$^F_4$] (**8**).

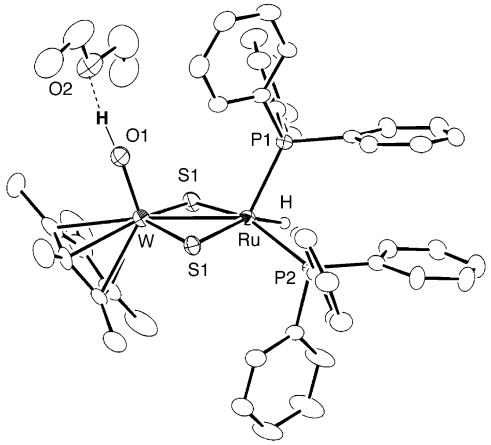

Figure 2. Structure of the complex cation of [Cp*W(OH)(μ-S)$_2$RuH(PPh$_3$)$_2$](BAr$^F_4$)·2C$_4$H$_{10}$O (**7a**·2C$_4$H$_{10}$O). The hydrogen atom bound to Ru was crystallographically located, whereas the hydroxyl hydrogen is added at an appropriate position in the figure in order to emphasize the hydrogen bonding with the ether molecule.

Complexes **7a** and **8** were characterized spectroscopically, and the structure of **7a** was determined by crystallographic analysis. Their ^{1}H NMR spectra show resonances for W−OH and Ru−H at δ 9.07 and −3.37 for **7a**, and at δ 5.69 and δ −3.98 for **8**. Disappearance of the characteristic ν(W═O) band and appearance of a ν(Ru−H) band at 2019 cm^{-1} and a ν(O−H) band at 3453 cm^{-1} in the IR spectrum of **7a** also agree with the formation of the W−OH and Ru−H moieties. As in the case of **5b**, two phosphines in **7a** and **8** are equivalent in the ^{31}P{^{1}H} NMR spectra at room temperature, due to a facile site exchange at Ru.

Single crystals of [Cp*W(OH)(μ-S)$_2$RuH(PPh$_3$)$_2$][BAr$^F_4$] (**7a**) suitable for X-ray diffraction study were obtained from an ether solution at −78 °C. The complex was crystallized with ether molecules as solvent of crystallization, and there was no short contact between the complex cation and the BAr$^F_4$ anion. Each ether molecule is situated in the neighborhood of the hydroxyl group of the complex cation, with O−O separation of 2.58 Å, indicating the WOH−O(ether) hydrogen bonding. The cation of **7a** with the hydrogen-bonded ether is shown in Figure 2, and the selected geometrical parameters are listed in Table 2.

(15) Kawaguchi, H.; Tatsumi, K., unpublished result.
(16) (a) O'Regan, M. B.; Liu, A. H.; Finch, W. C.; Schrock, R. R.; Davis, W. M. *J. Am. Chem. Soc.* **1990**, *112*, 4331. (b) Brunet, N.; Legzdins, P.; Trotter, J.; Yee, V. C. *Acta Crystallogr. Sect. C*, **1995**, *51*, 193. (c) Cao, R.; Tatsumi, K. *Inorg. Chem.* **2002**, *41*, 4102.
(17) Crabtree, R. H. In *The Organometallic Chemistry of The Transition Metals*, 2nd ed.; Wiley & Sons: New York, 1994.
(18) Brookhart, M.; Grant, B.; Volpe, J. *Organometallics* **1992**, *11*, 3920.

Scheme 3

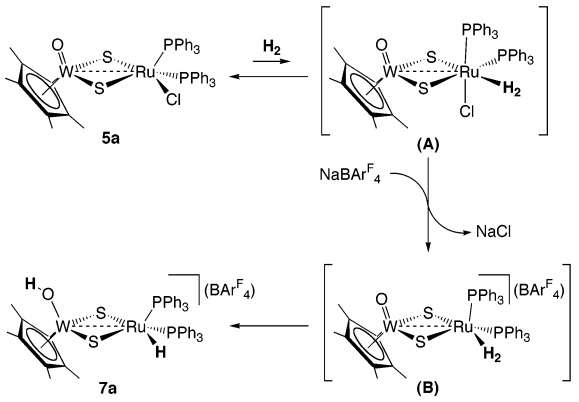

The dinuclear core geometry is very similar to those of Cp*W(O)(μ-S)$_2$RuH(PPh$_3$)$_2$ (**5b**), except for the W−O distance. The W−O bond length of 1.829(4) Å is substantially longer than the W═O distance of 1.746(4) Å in **5a**, which confirms that the oxygen atom attached to W is no longer a terminal oxo ligand but a hydroxyl group. It may be worth noting that the W−S bond lengths of **7a** are slightly shorter by 0.030 Å (av.) than those of **5a**. The shortening of the W−S bonds reflects the lesser extent of π donaton to W from the hydroxy ligand than that from oxo ligand, thereby allowing stronger π donation from the bridging sulfides.

Intriguingly, neither Cp*W(O)(μ-S)$_2$RuCl(PPh$_3$)$_2$ (**5a**) nor Cp*W(NPh)(μ-S)$_2$RuCl(PPh$_3$)$_2$ (**6a**) reacts with NaBAr$^F_4$ alone under N_2. As was mentioned earlier, **5a** (and **6a**) does not react with H_2 in the absence of NaBAr$^F_4$, even under 10 atm H_2. Thus both NaBAr$^F_4$ and H_2 must be present for the reaction to proceed, although the H_2 activation by **5a** and **6a** would presumably occur after the removal of chloride from the Ru site. The salt NaBAr$^F_4$ does not react with H_2 under this condition. In contrast, the tris(μ-sulfido) complex Cp*W(μ-S)$_3$RuCl(PPh$_3$)$_2$ (**4a**) reacts readily with NaBAr$^F_4$ in the absence of H_2 to give a dark brown solid. Although we were unable to characterize the dark brown product, it is interesting to note that the reaction of **4a** with NaBAr$^F_4$ under atmospheric H_2 produces a solid, the ^{1}H NMR spectrum of which is very similar to that of the above dark brown product. The difference between **4a** and **5a** is the coordination number of Ru, and the chloride at the octahedral Ru seems to be more labile. Taking these observations into account, we propose that the reaction of **5a** with NaBAr$^F_4$/H_2 is initiated by coordination of H_2 to the pentacoordinate Ru as shown in Scheme 3. The resulting octahedral H_2 complex, designated as (**A**) in Scheme 3, would have facilitated dissociation of chloride in the reaction with NaBAr$^F_4$. Removal of chloride from **A** leads to the square-pyramidal intermediate with η^2-H_2 (**B**), and subsequently the H_2 molecule splits into the Ru−H and W−OH forms in **7a**. Formation of η^2-H_2 complexes prior to the heterolytic H_2 cleavage has occasionally been speculated.[3b,4, 5c] The mechanism of the H_2-splitting process from **B** to **7a** will be discussed below.

Protonation Reactions of the Hydride Complexes. The hydridic centers of transition metal complexes often react with protons (H^+), and evolve H_2. Contrary to this preconception, we found the oxo ligand of Cp*W(O)(μ-S)$_2$RuH(PPh$_3$)$_2$ (**5b**) to be protonated when it was treated in THF with an equimolar amount of [H(OEt$_2$)$_2$][BAr$^F_4$] or HOTf. [Cp*W(OH)(μ-S)$_2$RuH(PPh$_3$)$_2$][BAr$^F_4$] (**7a**) and [Cp*W(OH)(μ-S)$_2$RuH(PPh$_3$)$_2$](OTf)

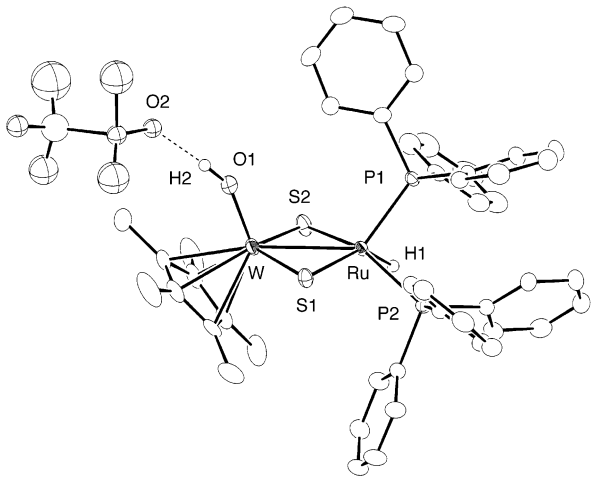

Figure 3. Structure of [Cp*W(OH)(μ-S)$_2$RuH(PPh$_3$)$_2$](OTf) (**7b**). The hydrogen bound to Ru was located by the X-ray analysis, and the hydroxyl hydrogen was put at a calculated position.

(**7b**) were isolated in 97% and 87% yields, respectively. In these reactions, the hydridic site at Ru remained intact, and no H_2 evolution was observed. Conversion of **7b** into **7a** was successful on anion exchange with NaBAr$^F_4$ in CH_2Cl_2. The occurrence of protonation at the oxo ligand points to two significant aspects: a) W═O is a more basic site than Ru−H, and b) the OH hydrogen in **7a** or **7b** is acidic in character.

Scheme 4

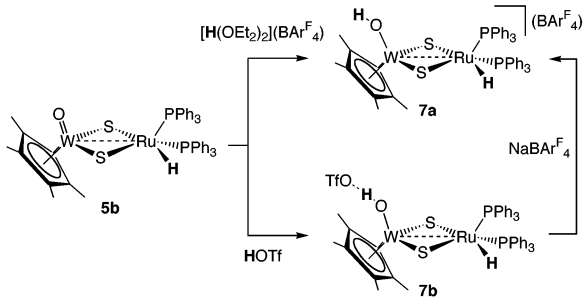

Complex **7b**, isolated as dark purple crystals, was characterized by spectroscopic data and by combustion analysis, and its structure was determined by X-ray analysis. The event of selective protonation at W═O was indicated by the disappearance of the characteristic ν(W═O) band, and by the persistence of the Ru−H band at 2015 cm^{-1} in the IR spectrum. Observation of ^{1}H NMR resonances at δ 10.8 (W−O*H*) and δ −5.96 (Ru-*H*) is consistent with the interpretation of the IR spectrum. Similar to **7a**, there appears a single peak in the ^{31}P{^{1}H} NMR spectrum at room temperature, and the two phosphine ligands are thus fluxional. The molecular structure of **7b** is presented in Figure 3, and selected bond lengths and angles are compared with those of **7a** in Table 2. The most notable feature of the crystal structure is the short contact between the W−OH group and the anion OTf$^-$. The O−O separation of 2.66(1) Å is indicative of hydrogen bonding. The W−O bond length of 1.858(4) Å is obviously elongated by protonation, as compared with the W═O bond of **5b**, and it is slightly longer than the W−OH distance of **7a**, too. The O−O separation is also longer for **7b** by 0.08 Å. The hydroxyl group of **7a** is hydrogen bonded to the ether oxygen, and the longer W−OH and O−O distances for **7b** suggest that the hydrogen bond with OTf$^-$ is weaker

Table 3. Selected Bond Distances (Å) and Angles (deg) for $[Cp^*W(\mu\text{-}S)_3RuL(PPh_3)_2](OTf)$ (L = CH_3CN (**9**), Co (**10**))

9				**10**			
W−Ru	2.6264(3)	W−S1−Ru	68.90(2)	W−Ru	2.660(1)	W−S1−Ru	68.5(1)
W−S1	2.2269(8)	W−S2−Ru	66.90(2)	W−S1	2.226(3)	W−S2−Ru	68.38(10)
W−S2	2.2306(9)	W−S3−Ru	67.17(2)	W−S2	2.207(4)	W−S3−Ru	66.40(10)
W−S3	2.2215(8)			W−S3	2.226(4)		
Ru−S1	2.4084(8)			Ru−S1	2.493(4)		
Ru−S2	2.5148(8)			Ru−S2	2.498(4)		
Ru−S3	2.5069(8)			Ru−S3	2.491(4)		
Ru−N	2.046(3)			Ru−C	1.86(2)		

than the interaction with ether. The coordination geometries at W and Ru resemble those of **5b** and **7a**.

In contrast to the selective protonation at the oxo ligand of **5b**, the analogous reaction of HOTf with $Cp^*W(\mu\text{-}S)_3RuH(PPh_3)_2$ (**4b**) occurred at the hydride site. Addition of HOTf to a THF solution of **4b** at room temperature caused an immediate evolution of H_2 to afford a dark red solution. Although the dark red product has not been characterized, it is presumed to be a cationic THF complex $[Cp^*W(\mu\text{-}S)_3Ru(THF)(PPh_3)_2][OTf]$, because a CH_3CN-adduct $[Cp^*W(\mu\text{-}S)_3Ru(CH_3CN)(PPh_3)_2][OTf]$ (**9**) and a CO-adduct $[Cp^*W(\mu\text{-}S)_3Ru(CO)(PPh_3)_2][OTf]$ (**10**) were isolated upon treating the dark red solution with CH_3CN and CO, respectively. The IR spectrum of **9** exhibits bands for CH_3CN at 2210 cm^{-1}, and for OTf^- at 1270, 1220, 1150, and 636 cm^{-1}, while complex **10** was characterized by a strong CO band at 1990 cm^{-1}. Their ^1H NMR spectra agree with the formulation, and the signal for free CH_3CN appeared for **9**, when the measurement was performed in CD_3CN. The structures of **9** and **10** were confirmed by crystallographic analysis, and the selected bond lengths and angles are given in Table 3. Similar to the molecular structures of $Cp^*W(\mu\text{-}S)_3RuX(PPh_3)_2$ (**4a**; X = Cl, **4b**; X = H), the two metal centers are bridged by three sulfides, and CH_3CN or CO is coordinated at Ru. A notable difference in the structures of **4a**, **4b**, **9**, and **10** is the Ru−S1 bond lengths trans to chloride (2.4079(7) Å), hydride (2.5387(8) Å), CH_3CN (2.4084(8) Å), and CO (2.493(4) Å), which show the strong trans influence of hydride and CO.

Scheme 5

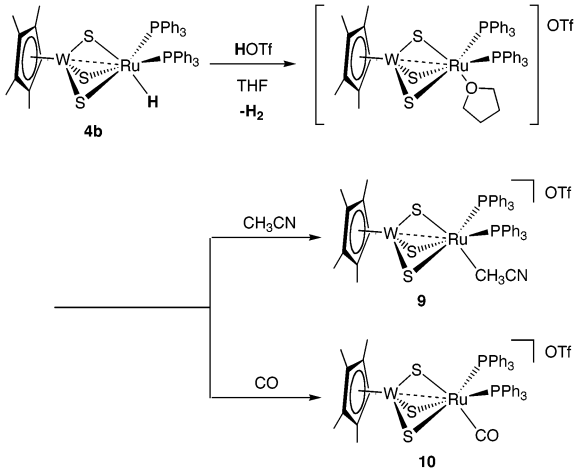

Deprotonation and H_2 Evolution. Addition of hydrogen at the oxo ligand can be accomplished either by the heterolytic cleavage of H_2 or by protonation. In expectation of obtaining insights into the mechanism of heterolytic H_2 activation, the reverse processes of H−H cleavage and protonation were investigated. The protic character of the WOH hydrogen was established by the observation that "deprotonation" of the complex cation $[Cp^*W(OH)(\mu\text{-}S)_2RuH(PPh_3)_2]^+$ (**7a**,**b**) was induced selectively by a small excess of NEt_3, resulting in quantitative formation of $Cp^*W(O)(\mu\text{-}S)_2RuH(PPh_3)_2$ (**5b**). Evolution of H_2, which would produce $[Cp^*W(O)(\mu\text{-}S)_2Ru(NEt_3)(PPh_3)_2]^+$, did not take place in this reaction.

Scheme 6

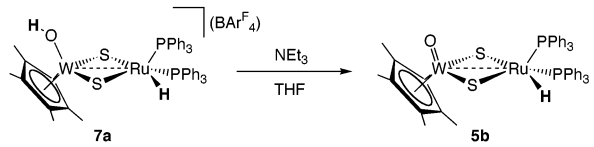

Scheme 7

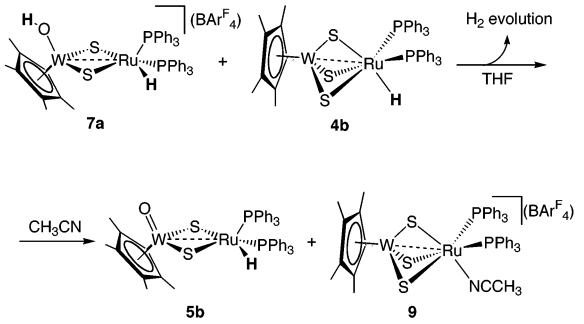

We mentioned earlier in this paper that the hydride of $Cp^*W(\mu\text{-}S)_3RuH(PPh_3)_2$ (**4b**) reacted readily with HOTf. Transition metal hydrides are potential bases, and could interact with the acidic W−OH group. As a matter of fact, treatment of $Cp^*W(\mu\text{-}S)_3RuH(PPh_3)_2$ (**4b**) with **7a** in THF resulted in immediate evolution of H_2, and the subsequent addition of CH_3CN into the resulting dark-brown solution produced **5b** and $[Cp^*W(\mu\text{-}S)_3Ru(CH_3CN)(PPh_3)_2][BAr^F{}_4]$ (**9**). Obviously H_2 was formed by an intermolecular coupling of the hydroxyl hydrogen in **7a** and the hydride in **4b**. This facile H_2 formation raises the intriguing question as to why **7a** or **7b** does not evolve H_2 by itself via an intermolecular or intramolecular H−H coupling pathway. They are stable in THF under an inert atmosphere. Hydridic character of the Ru−H bond may be weak, and/or the hydrogen bonding with OTf^- or ether may decrease the acidity of the hydroxyl hydrogen.

Although the complex cation $[Cp^*W(OH)(\mu\text{-}S)_2RuH(PPh_3)_2]^+$ is stable in THF, it was found to be labile in the presence of CH_3CN or under CO atmosphere. Upon addition of CH_3CN to a THF solution of **7a** or **7b**, the complex was gradually converted into $[Cp^*W(O)(\mu\text{-}S)_2Ru(CH_3CN)(PPh_3)_2](X)$ (**11a**;

Table 4. Selected Bond Distances (Å) and Angles (deg) for $[Cp^*W(O)(\mu\text{-}S)_2Ru(CH_3CN)(PPh_3)_2](OTf)$ (**11b**)

	11b
W−Ru	2.8603(3)
W−O	1.727(3)
W−S1	2.2644(9)
W−S2	2.2650(9)
Ru−S1	2.3648(9)
Ru−S2	2.3354(8)
Ru−N	2.063(3)
W−S1−Ru	76.65(3)
W−S2−Ru	76.87(3)

X = BAr^F_4, **11b**; X = OTf) with evolution of H_2. The product was isolated as a grayish blue crystalline powder in 95% yield. Formation of H_2 was detected by a separate NMR tube experiment in THF-d_8 with a small amount of CH_3CN, where the free H_2 signal appeared at δ 4.55. Complexes **11a** and **11b** were characterized by the IR bands associated with the W═O bond and CH_3CN, and by ^1H and $^{31}P\{^1H\}$ NMR spectra. As in the case of **5a**, the two phosphine ligands are chemically nonequivalent in the ^{31}P NMR spectrum. Crystals suitable for X-ray analysis were grown by layering ether onto a THF solution of **11b**. The X-ray derived geometric parameters are listed in Table 4. There is no short contact between the complex cations and the anions in the crystals. The dinuclear structure of the complex cation is analogous to those of **5a** and **5b**, in which the Ru atom adopts a distorted square pyramidal coordination geometry with an apical PPh_3, and with one PPh_3, two μ-S atoms, and one CH_3CN molecule at the basal positions.

Scheme 8

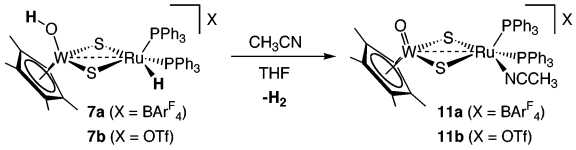

H/D Exchange Experiments. In the previous section, we mentioned that the hydride complex $Cp^*W(O)(\mu\text{-}S)_2RuH(PPh_3)_2$ (**5b**) appeared not to react under 10 atm H_2. To ascertain if **5b** is really inert to external H_2, an H/D exchange reaction was conducted in an NMR tube at room temperature, and the reaction was monitored by ^1H NMR. Introduction of D_2 onto a C_6D_6 solution of **5b** gave rise to $Cp^*W(O)(\mu\text{-}S)_2RuD(PPh_3)_2$ (**5b-*d***). Formation of HD and H_2 was noted in the ^1H NMR. The reaction is relatively slow and is nearly completed in 1 day. The exchange between D_2 and the hydride is most likely to proceed through coordination of η^2-D_2. The tri(μ-sulfido) hydride complex $Cp^*W(\mu\text{-}S)_3RuH(PPh_3)_2$ (**4b**) was also found to undergo the H/D exchange between the hydride and 1 atm D_2 to produce $Cp^*W(\mu\text{-}S)_3RuD(PPh_3)_2$ (**4b-*d***).

The NMR tube experiments were also carried out for the H/D exchange reactions of $[Cp^*W(OH)(\mu\text{-}S)_2RuH(PPh_3)_2][BAr^F_4]$ (**7a**). Surprisingly, exposure of a THF-d_8 solution of **7a** to D_2 lead to a facile exchange of *both* hydridic center attached to Ru and protic center on the OH group, giving rise to $[Cp^*W(OD)(\mu\text{-}S)_2RuD(PPh_3)_2][BAr^F_4]$ (**7a-d$_2$**) within 1 day, and the formation of HD and H_2 was identified in the ^1H NMR spectrum. More surprisingly, the treatment of **7a** with CH_3OD also resulted in **7a-d$_2$**. The deuterated complex **7a-d$_2$** was synthesized in a preparative scale by the reaction of **5a** with

Scheme 9

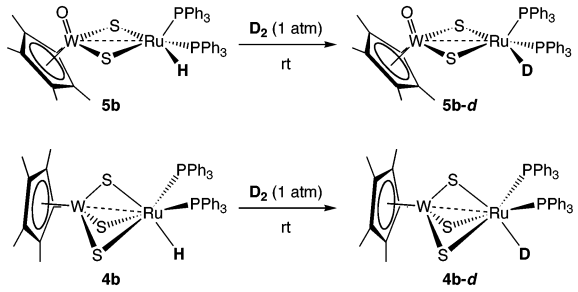

$NaBAr^F_4$ under a D_2 atmosphere, and it was characterized by means of ^1H, ^2H, and ^{31}P NNR spectra. In either of the reactions with D_2 and CH_3OD in NMR tubes, the intensity of the W−OH signal (or the W−OD signal) remains nearly equal to that of the Ru−H signal (or Ru-D signal). In other words, during the H/D exchange, the W−OH and Ru−H proton signals decrease approximately at the same rate, and the situation is similar to the concomitant increases of the corresponding ^2H signals.

Scheme 10

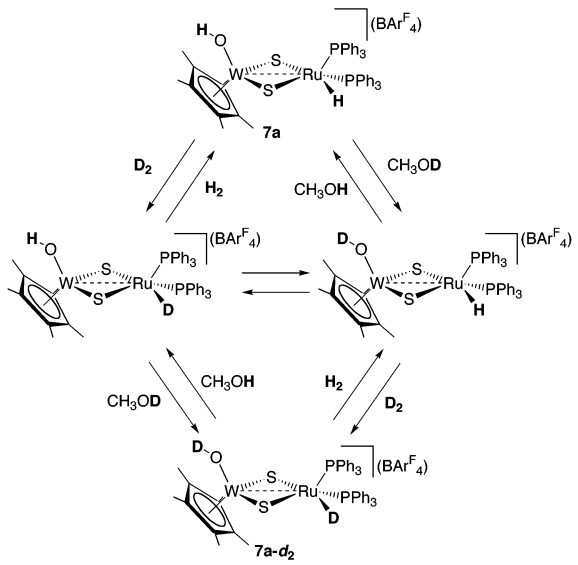

Scheme 11

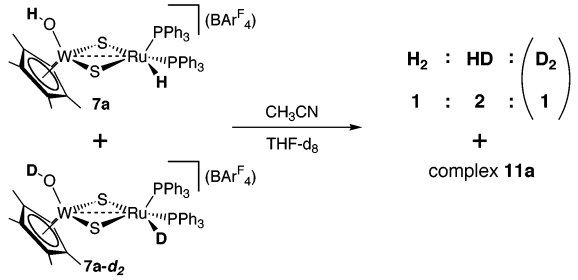

As one might expect, CH_3OD does not react with the hydride of $Cp^*W(O)(\mu\text{-}S)_2RuH(PPh_3)_2$ (**5b**). It may also be expected that a fast exchange between W−OH and D_2 is unlikely to proceed. Therefore, we propose that the H/D exchange at the W−OH site of **7a** under D_2 is actually initiated by deuteration of the hydride at Ru via D_2 coordination, and the H/D scramble between the W−OH and Ru-D sites follows. Likewise, in the reaction between **7a** and CH_3OD, deuteration probably occurs first at W−OH, which would then scramble over the two sites.

Scheme 12

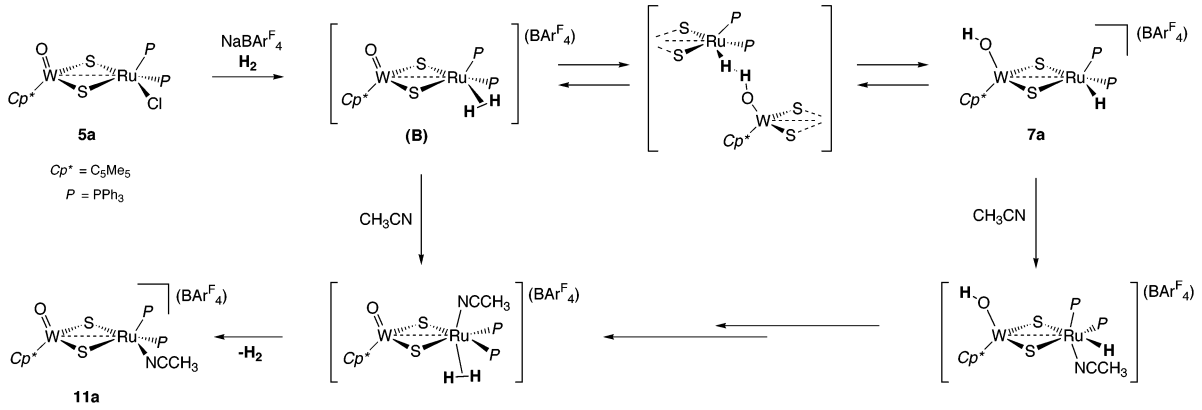

Scheme 13

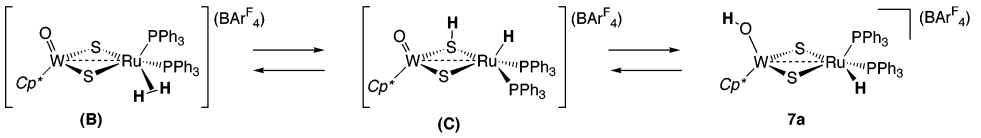

Since the H/D exchanges occur simultaneously at W−OH and Ru−H in the ^{1}H NMR time scale, the H(D) scramble between these sites must be much faster than the deuteration processes at Ru−H with D_2 and at W−OH with CH_3OD.

We have carried out a crossover experiment for the $H_2(D_2)$ formation from [Cp*W(OH)(μ-S)$_2$RuH(PPh$_3$)$_2$][BAr$^F_4$] (**7a**) and [Cp*W(OD)(μ-S)$_2$RuD(PPh$_3$)$_2$][BAr$^F_4$] (**7a-d$_2$**) in the presence of CH_3CN (see Scheme 11). In an NMR tube, a 1:1 mixture of **7a** and **7a-d$_2$** was dissolved in THF-d_8 and one drop of CH_3CN was added, followed by immediate ^{1}H NMR measurement. The spectrum clearly shows the signals of H_2 and HD in the 1:2 intensity ratio, and also points to the quantitative formation of [Cp*W(O)(μ-S)$_2$Ru(CH_3CN)(PPh$_3$)$_2$][BAr$^F_4$] (**11a**). If the H_2 evolution occurs within each molecule of **7a** and **7a-d$_2$**, H_2 and D_2 would be produced. On the other hand, if the reaction proceeds via an intermolecular pathway, a statistical amount of HD would also be generated, which is in accord with the experimental result. However, the formation of HD may also be explained in terms of a facile intermolecular/intramolecular H/D scrambling between **7a** and **7a-d$_2$** before the H_2 evolution. This possibility could not be ruled out.

Mechanistic Aspects of the Reversible H_2 Activation. We emphasized in Scheme 3 that the H_2 activation reaction of Cp*W(O)(μ-S)$_2$RuCl(PPh$_3$)$_2$ (**5a**) with NaBAr$^F_4$ could be initiated by formation of an η^2-H_2 complex Cp*W(O)(μ-S)$_2$RuCl(H_2)(PPh$_3$)$_2$ (**A**), and that dissociation of chloride from the intermediate, leading to another η^2-H_2 intermediate [Cp*W(O)(μ-S)$_2$Ru(H_2)(PPh$_3$)$_2$](BAr$^F_4$) (**B**), would then be facilitated by NaBAr$^F_4$. In this section, the mechanism of the subsequent H_2 splitting process of **B** to give [Cp*W(OH)(μ-S)$_2$RuH(PPh$_3$)$_2$](BAr$^F_4$) (**7a**) is discussed (Scheme 12). This process can be reversible, which would account for the mechanisms of H/D exchange reactions of **7a** (and **7b**) and facile H_2 evolution in CH_3CN to generate [Cp*W(O)(μ-S)$_2$Ru(CH_3CN)(PPh$_3$)$_2$](BAr$^F_4$) (**11a**). An alternative mechanism of the H_2 evolution is also implicated at the bottom of Scheme 12, where addition of CH_3CN to Ru of **7a** precedes the H−H coupling.

It has been known that the enhanced acidity of molecular hydrogen bound to electron deficient transition metal centers results in heterolytic H−H bond splitting. A proton is transferred to a counteranion, an external base, or to a basic site within the molecule. In the η^2-H_2 intermediate (**B**), the oxo group, the bridging sulfides, and the counteranion [BAr$^F_4$]$^-$ may act as proton acceptors. However, proton abstraction by [BAr$^F_4$]$^-$ is unlikely to occur, because a proton is only lost when a conjugate base such as Et_2O or H_2O is present to give [H(OEt_2)$_2$](BAr$^F_4$) or [H_3O](BAr$^F_4$), while the reaction of **5a** with H_2 was carried out in CH_2Cl_2. A direct intramolecular proton abstraction by W═O is also ruled out, because the W═O group is far away from the Ru coordination sphere.

Thus a plausible pathway for the H_2 activation is the one involving an intermolecular H−H splitting as shown in Scheme 12. This mechanism is analogous to the known deprotonation reactions of metal-bound η^2-H_2 molecules promoted by external bases. Another way to view this mechanism is that the reaction proceeds via the intermediate having an intermolecular interaction between the hydridic Ru−H site and the protic W−OH site. This Ru−H−H−O−W interaction is relevant to the so-called nonclassical hydrogen-bonding found in some transition metal hydride complexes,[19] e.g., the Ir−H−H−N interaction in [Ir{H(η^1-SC_5H_4NH)}$_2$(PCy$_3$)$_2$]BF$_4$[4a] and the Ir−H−H−O interaction observed in [Ir(H)$_2$\{(C_9H_6N)NC(OH)Me\}(PPh$_3$)$_2$](SbF$_6$).[4b]

On the other hand, a possibility of proton migration over the μ-S sites, by way of the μ-SH intermediate [Cp*W(O)(μ-S)(μ-SH)RuH(PPh$_3$)$_2$](BAr$^F_4$) (**C**), is not ruled out (Scheme 13). The bridging sulfide in (**B**) is in close vicinity to the molecular hydrogen at Ru, a lone pair of which is capable of abstracting a proton from the η^2-H_2 molecule. The resulting mercapto group is acidic, and would deriver the proton readily to the more basic oxo group. The heterolytic cleavage of H_2 by dinuclear μ-sulfido complexes have been reported to generate a μ-SH bond and a M−H bond.[6b,c,d]

(19) (a) Crabtree, R. H.; Siegbahn, P. E. M.; Eisenstein, O.; Rheingold, A. L.; Koetzle, T. *Acc. Chem. Res.* **1996**, *29*, 348, and references therein. (b) Stevens, R. C.; Bau, R.; Milstein, D.; Blum, O.; Koetzle, T. F. *J. Chem. Soc., Dalton Trans.* **1990**, 1429.

Experimental Section

General Procedures. All reactions and the manipulations of air-sensitive compounds were performed under nitrogen or argon atmosphere using standard Schlenk techniques. Solvents were dried, degassed and distilled from sodium/benzophenone ketyl (hexane, Et_2O, toluene, DME, THF) or from CaH_2 (CH_3CN, CH_2Cl_2) under nitrogen. Deuterated solvents were vacuum-transferred from sodium (benzene-d_6, toluene-d_8, THF-d_8) or CaH_2 (CD_3CN, CD_2Cl_2, $CDCl_3$).

^1H and ^{31}P NMR spectra were acquired on a Varian INOVA-500 spectrometer at 500 and 202 MHz, respectively. ^1H NMR spectra were referenced to the residual proton resonances of the deuterated solvents. ^{31}P chemical shifts were relative to the external reference of 85% H_3PO_4. Infrared spectra were recorded on a Parkin Elmer 2000 FT-IR spectrometer or a JASCO A3 spectrometer. ESI-MS spectra were obtained from a Perkin-Elmer Sciex API 300 ion spray mass spectrometer or a Micromass LCT TOF-MS spectrometer. Elemental analyses for C, H, N, and S were performed on a LECO CHNS-932 elemental analyzer where the crystalline samples were sealed in silver capsules under argon. FAB-MS spectra were obtained on a JEOL JMS-LCMATE mass spectrometer, where 3-nitrobenzyl alcohol was used as the matrix. X-ray diffraction data were collected on a Rigaku RASA-7 Quantum system and a Rigaku AFC7R equipped with an ADSC Quantum1 CCD detector by using graphite-monochromated MoKα radiation.

The following compounds were prepared according to the literature procedures. $(PPh_4)[Cp^*W(S)_3]$ (**1**),[10a] $(PPh_4)[Cp^*W(S)_2(O)]$ (**2**),[10b] $RuCl_2(PPh_3)_3$, $RuClH(PPh_3)_3$,[12] $NaBAr^F_4$ and $[H(OEt_2)_2]BAr^F_4$.[18]

Synthesis of $(PPh_4)[Cp^*W(S)_2(NPh)]$ (3). $(PPh_4)[Cp^*W(O)(S)_2]$ (**2**; 110 mg, 0.15 mmol) was dissolved in CH_3CN (15 mL) under nitrogen atmosphere, to which PhNCO (17 mL, 0.16 mmol) was added with stirring at 40 °C, and the reaction mixture was kept stirring for 2 h. The CH_3CN was removed under vacuum, and the residue was washed with hexane to give $(PPh_4)[Cp^*W(S)_2(NPh)]$ (**3**) as an orange powder (118 mg, 98%). ^1H NMR (CD_3CN): δ 8.0−7.6 (m, 20 H, PPh_4), 7.21−6.70 (m, 5 H, NPh), 1.99 (s, 15 H, Cp*). IR (KBr pellet): 1350 (s, W═NPh), 455, 434 (s, W═S) cm^{-1}. ESI-MS (CH_3CN): *m*/*z* 474 ($[Cp^*W(S)_2(NPh)]^-$). Anal. Calcd for $C_{40}H_{40}NS_2PW$: C 59.04; H 4.95; N 1.72; S 7.88 Found: C 58.27; H 5.16; N 1.76; S 7.85.

Synthesis of $Cp^*W(\mu\text{-}S)_3RuCl(PPh_3)_2$ (4a). A mixture of $(PPh_4)[Cp^*W(S)_3]$ (**1**) (0.37 g, 0.50 mmol) and $RuCl_2(PPh_3)_3$ (0.47 g, 0.49 mmol) in CH_3CN (60 mL) was stirred at room temperature for 4 h. After removal of the solvent under vacuum, the black-brown residue was washed with THF (20 mL) and CH_3CN (40 mL) to afford $Cp^*W(\mu\text{-}S)_3RuCl(PPh_3)_2$ (**4a**) as a brown powder (0.41 g, 77%). X-ray quality crystals were grown by layering hexane onto the CH_2Cl_2 solution of **4a** at room temperature. ^1H NMR ($CDCl_3$): δ 7.48−7.45 (m, 12 H, PPh_3), 7.23−7.20 (m, 6 H, PPh_3), 7.10−7.06 (m, 12 H, PPh_3), 2.10 (s, 15 H, Cp*). $^{31}P\{^1H\}$ NMR ($CDCl_3$): δ 31.7 (s, PPh_3). Anal. Calcd for $C_{46}H_{45}ClP_2RuS_3W\cdot CH_2Cl_2$: C, 48.61; H, 4.08; S, 8.28. Found: C, 48.29; H, 4.14, S, 8.54.

Synthesis of $Cp^*W(\mu\text{-}S)_3RuH(PPh_3)_2$ (4b). CH_3CN (120 mL) was added to a mixture of $(PPh_4)[Cp^*W(S)_3]$ (**1**) (1.21 g, 1.61 mmol) and $RuClH(PPh_3)_3$ (1.59 g, 1.56 mmol). The suspension was stirred at room temperature for 1 day to yield brown precipitation. After decanting brown solution off, the brown residue was extracted with toluene (80 mL), and centrifuged to remove PPh_4Cl. After removal of the solvent in vacuo, the brown residue was washed with CH_3CN (30 mL) to afforded $Cp^*W(\mu\text{-}S)_3RuH(PPh_3)_2$ (**4b**) as a brown crystalline powder (1.35 g, 83%). X-ray quality crystals were grown by layering hexane onto the toluene solution of **4b** at room temperature. ^1H NMR ($CDCl_3$): δ 7.53−7.49 (m, 12H, PPh_3), 7.15−7.02 (m, 18 H, PPh_3), 2.06 (s, 15 H, Cp*), −10.47 (t, $^2J_{PH}$ = 29 Hz, 1 H, RuH). $^{31}P\{^1H\}$ NMR ($CDCl_3$): δ 57.3 (s, PPh_3). ^1H NMR (C_6D_6): δ 7.88−7.85 (m, 12 H, PPh_3), 7.00−6.94 (m, 18 H, PPh_3), 1.91 (s, 15 H, Cp*), −10.30 (t, $^2J_{PH}$ = 30 Hz, 1 H, RuH). $^{31}P\{^1H\}$ NMR (C_6D_6): δ 58.5 (s, PPh_3). IR (Nujol): 1930 (w, n_{Ru-H}) cm^{-1}. Anal. Calcd for $C_{46}H_{46}P_2RuS_3W$: C, 53.02; H, 4.45; S, 9.23. Found: C, 52.82; H, 4.52, S, 9.18.

Synthesis of $Cp^*W(O)(\mu\text{-}S)_2RuCl(PPh_3)_2$ (5a). The procedure is similar to the one used for the synthesis of **4a**. The reaction of $(PPh_4)[Cp^*W(S)_2(O)]$ (**2**) (0.94 g, 1.27 mmol) with $RuCl_2(PPh_3)_3$ (1.21 g, 1.27 mmol) in CH_3CN (125 mL) gave $Cp^*W(O)(\mu\text{-}S)_2RuCl(PPh_3)_2$ (**5a**) as a green powder (1.10 g, 82%). X-ray quality crystals were grown from hexane/CH_2Cl_2 at room temperature. ^1H NMR ($CDCl_3$): δ 7.28−7.00 (m, 30 H, PPh_3), 1.88 (s, 15 H, Cp*). $^{31}P\{^1H\}$ NMR ($CDCl_3$): δ 68.8 (d, $^2J_{PP}$ = 30 Hz, PPh_3), 26.4(d, $^2J_{PP}$ = 30 Hz, PPh_3). IR (Nujol): 895 (s, $\nu_{W=O}$) cm^{-1}. Anal. Calcd for $C_{46}H_{45}ClOP_2RuS_2W\cdot CH_2Cl_2$: C, 49.29; H, 4.14; S, 5.60. Found: C, 48.81; H, 4.30; S, 5.46.

Synthesis of $Cp^*W(O)(\mu\text{-}S)_2RuH(PPh_3)_2$ (5b). The synthetic procedure is analogous to that of **4b**. The reaction of $(PPh_4)[Cp^*W(S)_2(O)]$ (**2**) (0.97 g, 1.32 mmol) with $RuClH(PPh_3)_3$ (1.31 g, 1.28 mmol) in CH_3CN (125 mL) afford $Cp^*W(O)(\mu\text{-}S)_2RuH(PPh_3)_2$ (**5b**) as a greenish brown crystalline powder (1.14 g, 86%). X-ray quality crystals were grown from a hexane/toluene solution at room temperature. ^1H NMR (C_6D_6): δ 7.64−7.60 (m, 12 H, PPh_3), 6.93−6.88 (m, 18 H, PPh_3), 1.86 (s, 15 H, Cp*), −8.17 (t, $^2J_{PH}$ = 33 Hz, 1 H, RuH). $^{31}P\{^1H\}$ NMR (C_6D_6): δ 68.5 (s, PPh_3). IR (Nujol): 2022 (w, ν_{Ru-H}), 901 (s, $\nu_{W=O}$) cm^{-1}. Anal. Calcd for $C_{46}H_{46}OP_2RuS_2W$: C, 53.83; H, 4.52; S, 6.25. Found: C, 53.98; H, 4.65; S, 6.54.

Synthesis of $Cp^*W(NPh)(\mu\text{-}S)_2RuCl(PPh_3)_2$ (6a). By following a procedure similar to that **4a**, the reaction of $(PPh_4)[Cp^*W(S)_2(NPh)]$ (**3**) (0.31 g, 0.38 mmol) with $RuCl_2(PPh_3)_3$ (0.36 g, 0.38 mmol) in CH_3CN (15 mL) gave $Cp^*W(NPh)(\mu\text{-}S)_2RuCl(PPh_3)_2$ (**6a**) as a green powder (0.23 g, 54%). ^1H NMR ($CDCl_3$): δ 7.30−6.98 (m, 30 H, PPh_3), 6.86 (brt, 2 H, NPh), 6.67 (brt, 1 H, NPh), 6.17 (brd, 2 H, NPh), 1.88 (s, 15 H, Cp*). $^{31}P\{^1H\}$ NMR ($CDCl_3$): δ 69.5 (d, $^2J_{PP}$ = 30 Hz, PPh_3), 26.4 (d, $^2J_{PP}$ = 30 Hz, PPh_3). IR (KBr pellet): 1336 (s, $\nu_{W=NPh}$) cm^{-1}. FAB-MS^+ (CH_2Cl_2): *m*/*z* 1135 ($[Cp^*W(NPh)(\mu\text{-}S)_2RuCl(PPh_3)_2]^+$), 1100 ($[Cp^*W(NPh)(\mu\text{-}S)_2Ru(PPh_3)_2]^+$), 873 ($[Cp^*W(NPh)(\mu\text{-}S)_2RuCl(PPh_3)]^+$), 838 ($[Cp^*W(NPh)(\mu\text{-}S)_2RuPPh_3]^+$). Anal. Calcd for $C_{52}H_{50}NP_2RuS_2W$: C, 55.00; H, 4.44; N, 1.23; S, 5.65. Found: C, 55.00; H, 4.69; N, 1.30; S, 5.63.

Synthesis of $Cp^*W(NPh)(\mu\text{-}S)_2RuH(PPh_3)_2$ (6b). The procedure is similar to that of **4b**. The reaction of $(PPh_4)[Cp^*W(S)_2(NPh)]$ (**3**) (0.34 g, 0.42 mmol) with $RuClH(PPh_3)_3$ (0.39 g, 0.42 mmol) in CH_3CN (10 mL) afford $Cp^*W(NPh)(\mu\text{-}S)_2RuH(PPh_3)_2$ (**6b**) as a brown powder (0.35 g, 76%). ^1H NMR (C_6D_6): δ 7.72−7.68 (m, 12 H, PPh_3), 7.46−7.40 (m, 1 H, NPh), 6.98−6.94 (m, 2 H, NPh), 6.92−6.88 (m, 6 H, PPh_3), 6.86−6.80 (m, 12 H, PPh_3), 6.76−6.74 (m, 2 H, NPh), 1.79 (s, 15 H, Cp*), −10.81 (t, $^2J_{PH}$ = 33 Hz, 1 H, Ru−H). $^{31}P\{^1H\}$ NMR (C_6D_6): δ 69.3 (s, PPh_3). IR (KBr pellet): 1348 (s, $\nu_{W=NPh}$) cm^{-1}.

Formation of $[Cp^*W(OH)(\mu\text{-}S)_2RuH(PPh_3)_2](BAr^F_4)$ (7a) from 5b, H_2 gas, and $NaBAr^F_4$. A mixture of **5b** (0.15 g, 0.14 mmol) and $NaBAr^F_4$ (0.13 g, 0.15 mmol) in CH_2Cl_2 (10 mL) was stirred under H_2 atmosphere (1 atm) at room temperature for 1 h. The solution quickly turned purple. After being centrifuged to remove NaCl, the solvent was removed under vacuum. The purple residue was washed with small amount of hexane to afford $[Cp^*W(OH)(\mu\text{-}S)_2RuH(PPh_3)_2](BAr^F_4)$ (**7a**) as a purple powder (0.23 g, 84%). The NMR, IR, and ESI-MS spectra were measured using this purple powder. X-ray quality crystals were grown by cooling an ether solution of **7a** at −78 °C. ^1H NMR (THF-d_8): δ 9.07 (brs, 1 H, WOH), 7.80 (br, 8 H, BAr^F_4), 7.58 (br, 4 H, BAr^F_4) 7.4−7.1 (m, 30 H, PPh_3), 1.99 (s, 15 H, Cp*), −3.37 (t, $^2J_{PH}$ = 32 Hz, 1 H, RuH). $^{31}P\{^1H\}$ NMR (THF-d_8): δ 70.8 (s, PPh_3). ^1H NMR ($CDCl_3$): δ 7.70 (br, 8 H, BAr^F_4), 7.50 (br, 4 H, BAr^F_4) 7.4−7.1 (m, 30 H, PPh_3), 1.93 (s, 15 H, Cp*), −1.70 (t, $^2J_{PH}$ = 32 Hz, 1 H, RuH). $^{31}P\{^1H\}$ NMR ($CDCl_3$): δ 67.1 (s, PPh_3). IR (KBr pellet): 3453 (m, ν_{WO-H}), 2019 (w, ν_{Ru-H}) cm^{-1}. ESI-MS (THF): *m*/*z* 1026 ($[Cp^*W(OH)(\mu\text{-}S)_2RuH(PPh_3)_2-H]^+$). Anal. Calcd for $C_{78}H_{59}BF_{24}OP_2RuS_2W\cdot C_4H_{10}O$: C, 50.14; H, 3.54; S, 3.26. Found: C, 50.07; H, 3.68; S, 3.09.

Formation of $[Cp^*W(NHPh)(\mu\text{-}S)_2RuH(PPh_3)_2](BAr^F_4)$ (8) from 6b, H_2 gas, and $NaBAr^F_4$. The procedure is analogous to that used for

Table 5. Crystal Data for Cp*W(μ-S)$_3$RuCl(PPh$_3$)$_2$·CH$_2$Cl$_2$ (**4a**·CH$_2$Cl$_2$), Cp*W(μ-S)$_3$RuH(PPh$_3$)$_2$ (**4b**), Cp*W(O)(μ-S)$_2$RuCl(PPh$_3$)$_2$·CH$_2$Cl$_2$ (**5a**·CH$_2$Cl$_2$), Cp*W(O)(μ-S)$_2$RuCl(PPh$_3$)$_2$·C$_6$H$_5$CH$_3$ (**5b**·C$_6$H$_5$CH$_3$), [Cp*W(OH)(μ-S)$_2$RuH(PPh$_3$)$_2$](BAr$^F_4$)·2C$_4$H$_{10}$O (**7a**·2C$_4$H$_{10}$O), [Cp*W(OH)(μ-S)$_2$RuH(PPh$_3$)$_2$]OTf (**7b**), [Cp*W(μ-S)$_3$RuL(PPh$_3$)$_2$](OTf) (L = CH$_3$CN (**9**), CO (**10**)), and [Cp*W(O)(μ-S)$_2$Ru(CH$_3$CN)(PPh$_3$)$_2$](OTf) (**11b**)

	4a•CH$_2$Cl$_2$	**4b**	**5a**•CH$_2$Cl$_2$	**5b**•C$_6$H$_5$CH$_3$
formula	C$_{46}$H$_{45}$ClP$_2$S$_3$RuW•CH$_2$Cl$_2$	C$_{46}$H$_{46}$P$_2$S$_3$RuW	C$_{46}$H$_{45}$ClP$_2$S$_2$ORuW•CH$_2$Cl$_2$	C$_{46}$H$_{46}$P$_2$S$_2$ORuW•C$_6$H$_5$CH$_3$
mol wt (g mol^{-1})	1161.29	1041.92	1145.23	1118.00
crystal system	orthorhombic	triclinic	orthorhombic	triclinic
space group	*Pbca* (No. 61)	$P\bar{1}$ (No.2)	*Pna*2$_1$ (No.33)	$P\bar{1}$ (No.2)
color of crystal	red	red	green	red
a (Å)	34.5808(3)	11.5969(8)	23.7028(5)	10.1719(5)
b (Å)	18.2206(1)	12.611(1)	14.8984(1)	12.1015(7)
c (Å)	14.4798(1)	16.3226(2)	12.9654(1)	19.543(1)
α (°)		84.380(1)		87.3157(6)
β (°)		75.862(3)		88.1864(9)
γ (°)		65.3699(7)		76.985(1)
V (Å^3)	9123.47(10)	2104.3(2)	4578.52(8)	2339.6(2)
Z	8	2	4	2
R	0.027	0.020	0.026	0.035
*R*w	0.052	0.022	0.042	0.055
GOF	1.81	1.00	2.02	1.89

	7a•2C$_4$H$_{10}$O	**7b**	**9**	**10**	**11b**
formula	C$_{78}$H$_{59}$F$_{24}$BP$_2$S$_2$ORuW·2C$_4$H$_{10}$O	C$_{47}$H$_{47}$F$_3$P$_2$S$_3$O$_4$RuW	C$_{49}$H$_{48}$F$_3$NP$_2$S$_4$O$_3$RuW	C$_{48}$H$_{45}$F$_3$P$_2$S$_4$O$_4$RuW	C$_{49}$H$_{48}$F$_3$NP$_2$S$_3$O$_4$RuW
mol wt (g mol^{-1})	2038.33	1175.93	1231.03	1217.98	1214.97
crystal system	triclinic	triclinic	triclinic	monoclinic	monoclinic
space group	$P\bar{1}$ (No.2)	$P\bar{1}$ (No.2)	$P\bar{1}$ (No.2)	*P*2$_1$/*c* (No.14)	*P*2$_1$/*n* (No.14)
color of crystal	purple	purple	red	orange	dark blue
a (Å)	13.929(1)	9.2932(6)	12.5670(6)	14.857(2)	12.9743(6)
b (Å)	14.281(2)	13.7152(7)	13.764(1)	16.402(3)	24.498(2)
c (Å)	23.637(3)	18.4144(6)	14.728(1)	22.9772(8)	14.9406(2)
α (°)	103.543(3)	104.7569(6)	77.6218(6)		
β (°)	104.860(1)	95.1659(1)	77.0646(5)	94.7078(8)	91.9160(3)
γ (°)	95.669(1)	91.219(1)	82.866(1)		
V (Å^3)	4354.7(7)	2258.0(2)	2417.4(2)	5580(1)	4746.2(3)
Z	2	2	2	4	4
R	0.058	0.042	0.028	0.075	0.028
*R*w	0.069	0.054	0.051	0.091	0.036
GOF	1.60	2.20	1.91	4.71	2.04

[a] $R = \Sigma||F_o| - |F_c||/\Sigma|F_o|$, $Rw = [\{\Sigma w(|F_o| - |F_c|)^2\}/\Sigma wF_o^2]^{1/2}$, GOF = $[\Sigma w(|F_o^2| - |F_c^2|)^2/(N_o - N_p)]^{1/2}$, where N_o and N_p denote the number of data and parameters.

the synthesis of **7a**. The reaction of Cp*W(NPh)(μ-S)$_2$RuCl(PPh$_3$)$_2$ (**6b**) (0.090 g, 0.079 mmol) with NaBAr$^F_4$ (0.070 g, 0.079 mmol) under H$_2$ atmosphere at room temperature gave [Cp*W(NHPh)(μ-S)$_2$RuH(PPh$_3$)$_2$](BAr$^F_4$) (**8**) as a dark-brown powder (0.148 g, 95%). ^{1}H NMR (THF-d$_8$): δ 7.80 (br, 8 H, BAr$^F_4$), 7.58 (br, 4 H, BAr$^F_4$) 7.4−7.0 (m, 30 H, PPh$_3$), 6.9−6.7 (m, 5 H, NPh) 5.69 (brs, 1 H, N*H*Ph), 1.74 (s, 15 H, Cp*), −3.98 (t, $^2J_{PH}$ = 32 Hz, 1H, RuH). ^{31}P{^{1}H} NMR (THF-d$_8$): δ 68.43 (s, PPh$_3$). IR (KBr pellet): 3303 (m, ν_{N-H}) cm^{-1}. ESI-MS (CH$_2$Cl$_2$): *m*/*z* 1103 ([Cp*W(NHPh)(μ-S)$_2$RuH(PPh$_3$)$_2$+H]$^+$). Anal. Calcd for C$_{84}$H$_{64}$BF$_{24}$NP$_2$RuS$_2$W: C, 51.34; H, 3.28; N, 0.71; S, 3.26. Found: C, 50.97; H, 3.59; N, 0.79; S, 2.83.

Reaction of Cp*W(O)(μ-S)$_2$RuH(PPh$_3$)$_2$ (5b) with [H(OEt$_2$)$_2$](BAr$^F_4$). A THF (5 mL) solution of [H(OEt$_2$)$_2$](BAr$^F_4$) (0.096 g, 0.095 mmol) was added to a solution of **5b** (0.10 g, 0.10 mmol) in THF (10 mL) with stirring at room temperature. The solution immediately turned purple and was stirred for 2 h. Solvent was removed under vacuum, and the purple residue was washed with a small amount of hexane to afford **7a** as a purple powder (0.19 g, 97%).

Formation of [Cp*W(OH)(μ-S)$_2$RuH(PPh$_3$)$_2$](OTf) (7b) from 5b and TfOH. Addition of TfOH (0.17 mmol) to a THF (20 mL) solution of **5b** (0.17 g, 0.17 mmol) formed a purple solution. The mixture was stirred at room temperature for 2.5 h. After removal of a solvent in vacuo, the purple residue was extracted with DME (3 mL). Then layering ether and hexane onto DME purple solution yields [Cp*W(OH)(μ-S)$_2$RuH(PPh$_3$)$_2$](OTf) (**7b**) as dark purple crystals (0.17 g, 87%). ^{1}H NMR (THF-d$_8$): δ 10.8 (brs, 1 H, WOH), 7.32−7.28 (m, 12 H, PPh$_3$), 7.24−7.21 (m, 6 H, PPh$_3$), 7.12−7.09 (m, 12 H, PPh$_3$), 1.95 (s, 15 H, Cp*), −5.96 (t, $^2J_{PH}$ = 32 Hz, 1 H, RuH). ^{31}P{^{1}H} NMR (THF-d$_8$): δ 68.9 (s, PPh$_3$). ^{1}H NMR (CDCl$_3$): δ 7.29−7.24 (m, 18 H, PPh$_3$), 7.14−7.11 (m, 12 H, PPh$_3$), 1.96 (s, 15 H, Cp*), −4.81 (t, $^2J_{PH}$ = 32 Hz, 1 H, RuH). ^{31}P{^{1}H} NMR (CDCl$_3$): δ 66.4 (s, PPh$_3$). IR (KBr pellet): 2015 (w, ν_{Ru-H}) cm^{-1}. Anal. Calcd for C$_{47}$H$_{47}$F$_3$O$_4$P$_2$RuS$_3$W: C, 48.00; H, 4.03; S, 8.18. Found: C, 48.23; H, 4.15; S, 8.22.

Anion exchange of [Cp*W(OH)(μ-S)$_2$RuH(PPh$_3$)$_2$](OTf) (7b) with NaBAr$^F_4$. A THF (30 mL) solution of NaBAr$^F_4$ (0.32 g, 0.36 mmol) was added to a THF (20 mL) solution of **7b** prepared from the reaction of **5b** (0.37 g, 0.36 mmol) with TfOH in situ at room temperature, and the reaction mixture was stirred for 20 min. Solvent was removed in vacuo, and the purple residue was extracted with CH$_2$Cl$_2$. After being centrifuged to remove NaCl, the purple solution was evaporated under vacuum. The purple residue was washed with hexane to yield **7a** as a purple powder (0.60 g, 88%).

Formation of [Cp*W(μ-S)$_3$Ru(CH$_3$CN)(PPh$_3$)$_2$](OTf) (9) from 4b, TfOH, and CH$_3$CN. Addition of TfOH (0.28 mmol) to a solution of **4b** (0.29 g, 0.28 mmol) in THF (40 mL) led to evolution of H$_2$. The mixture was stirred at room temperature for 2 h, and centrifuged. After removal of the solvent under vacuum, the brown residue was dissolved in CH$_3$CN (10 mL). The mixture was stirred at room temperature for 1 h. After removal of the solvent in vacuo, the brown residue was washed with DME (2 mL) to afford [Cp*W(μ-S)$_3$Ru(CH$_3$CN)(PPh$_3$)$_2$](OTf) (**9**) as a brown crystalline powder (0.30 g, 89%). X-ray quality crystals were grown by layering ether onto the DME/CH$_3$CN solution of **9** at room temperature. ^{1}H NMR (CD$_3$CN): δ 7.44−7.40 (m, 18 H, PPh$_3$), 7.31−7.28 (m, 12 H, PPh$_3$), 2.19 (s, 15 H, Cp*). 1.97 (s, 3 H, free CH$_3$CN). ^{31}P{^{1}H} NMR (CD$_3$CN): δ 37.5 (s, PPh$_3$). IR (Nujol): 2210 (w, ν_{CH3CN}) cm^{-1}. ESI-MS (CH$_3$CN): *m*/*z* 1082 ([Cp*W(μ-S)$_3$Ru-

$(CH_3CN)(PPh_3)_2]^+$), 1041 ($[Cp^*W(\mu\text{-}S)_3Ru(PPh_3)_2]^+$). Anal. Calcd for $C_{49}H_{48}F_3NO_3P_2RuS_4W$: C, 47.80; H, 3.93; N, 1.14; S, 10.42. Found: C, 47.52; H, 4.00; N, 1.14; S, 11.08.

Formation of [Cp*W(μ-S)$_3$Ru(CO)(PPh$_3$)$_2$](OTf) (10) from 4b, TfOH, and CO. After the reaction mixture of TfOH (0.35 mmol) and **4b** (0.36 g, 0.35 mmol) in THF (30 mL) was stirred at room temperature for 30 min, where generation of H_2 was noticed, CO (1 atm) was introduced and the solution was stirred for 2 h. The THF solution was concentrated, and addition of ether (50 mL) gave rise to an orange precipitation. After decantation, the orange solid was washed with ether to afford $[Cp^*W(\mu\text{-}S)_3Ru(CO)(PPh_3)_2](OTf)$ (**10**) as a orange powder (0.19 g, 46%). X-ray quality crystals were grown from hexane/THF at room temperature. ^1H NMR ($CDCl_3$): δ 7.44−7.38 (m, 6 H, PPh_3), 7.3−7.2 (m, 24 H, PPh_3), 2.27 (s, 15 H, Cp*). $^{31}P\{^1H\}$ NMR ($CDCl_3$): δ 37.2 (s, PPh_3). IR (Nujol): 1990 (w, ν_{CO}) cm^{-1}. ESI-MS (CH_3CN): *m*/*z* 1069 ($[Cp^*W(\mu\text{-}S)_3Ru(CO)(PPh_3)_2]^+$). Anal. Calcd for $C_{48}H_{45}F_3NO_4P_2RuS_4W$: C, 47.33; H, 3.72; S, 10.53. Found: C, 46.81; H, 4.05; S, 10.68.

Reaction of [Cp*W(OH)(μ-S)$_2$RuH(PPh$_3$)$_2$](BAr$^F_4$) (7a) with Et$_3$N. A resealable NMR tube was charged with a THF-d_8 (0.6 mL) solution of **7a** (0.039 g, 0.021 mmol), and one drop of Et_3N was added. The NMR tube was shaken repeatedly at room temperature, and immediately placed in the NMR spectrometer. The spectrum showed a quantitative formation of $Cp^*W(O)(\mu\text{-}S)_2RuH(PPh_3)_2$ (**5b**).

Reaction of [Cp*W(OH)(μ-S)$_2$RuH(PPh$_3$)$_2$](BAr$^F_4$) (7a) with Cp*W(μ-S)$_3$RuH(PPh$_3$)$_2$ (4b). A resaelable NMR tube containing the reaction mixture of **7a** (0.022 g, 0.012 mmol) and **4b** (0.012 g, 0.012 mmol) in THF-d_8 (0.6 mL) was shaken, and was set on an NMR spectrometer. Generation of H_2 and a quantitative amount of $Cp^*W(O)(\mu\text{-}S)_2RuH(PPh_3)_2$ (**5b**) was observed in the ^1H NMR spectrum together with uncharacterizable signals. Then, a small amount of CH_3CN was added to the solution. The NMR tube was shaken and was subjected for the NMR measurement. The resulting ^1H and $^{31}P\{^1H\}$ NMR spectra revealed a quantitative formation of $[Cp^*W(\mu\text{-}S)_3Ru(CH_3CN)(PPh_3)_2](BAr^F_4)$ (**9**) and **5b**.

Formation of [Cp*W(O)(μ-S)$_2$Ru(CH$_3$CN)(PPh$_3$)$_2$](BAr$^F_4$) (11a) from 7a and CH$_3$CN. To an ether (5 mL) solution of **7a** (0.122 g, 0.065 mmol) was added CH_3CN (0.1 mL) at room temperature. Evolution of H_2 was observed, and the resulting yellow solution was stirred for 10 min. The solvent was removed in vacuo, and the residue was washed with hexane to give $[Cp^*W(O)(\mu\text{-}S)_2Ru(CH_3CN)(PPh_3)_2](BAr^F_4)$ (**11a**) as a blue powder (0.118 g, 95%). ^1H NMR ($CDCl_3$): δ 7.70 (br, 8 H, BAr^F_4), 7.52 (br, 4 H, BAr^F_4), 7.4−6.8 (m, 30 H, PPh_3), 1.91 (s, 3 H, CH_3CN), 1.90 (s, 15 H, Cp*). $^{31}P\{^1H\}$ NMR ($CDCl_3$): δ 68.7 (d, $^2J_{PP}$ = 26 Hz, PPh_3), 32.8 (d, $^2J_{PP}$ = 26 Hz, PPh_3). IR (Nujol): 2279 (w, ν_{CH3CN}), 912 (s, $\nu_{W=O}$) cm^{-1}. ESI-MS (CH_2Cl_2): *m*/*z* 1066 ($[Cp^*W(O)(\mu\text{-}S)_2Ru(CH_3CN)(PPh_3)_2]^+$). Anal. Calcd for $C_{80}H_{60}BF_{24}NOP_2RuS_2W$: C, 49.81; H, 3.13; N, 0.73; S, 3.32. Found: C, 49.49; H, 3.30; N, 0.85; S, 3.22.

Formation of [Cp*W(O)(μ-S)$_2$Ru(CH$_3$CN)(PPh$_3$)$_2$](OTf) (11b) from 7b and CH$_3$CN. To a THF (50 mL) solution of **7b** prepared from the reaction between **5b** (0.36 g, 0.35 mmol) and TfOH in situ was added CH_3CN (3 mL) at room temperature. Evolution of H_2 was observed, and the resulting yellow solution was stirred for 2 h. The solvent was removed in vacuo, and yellow residue was washed with ether and toluene to give $[Cp^*W(O)(\mu\text{-}S)_2Ru(CH_3CN)(PPh_3)_2](OTf)$ (**11b**) as a blue powder (0.40 g, 95%). X-ray quality crystals were grown from ether/THF. ^1H NMR ($CDCl_3$): δ 7.46−6.88 (m, 30 H, PPh_3), 2.30 (s, 3 H, CH_3CN), 1.89 (s, 15 H, Cp*). $^{31}P\{^1H\}$ NMR ($CDCl_3$): δ 68.4 (d, $^2J_{PP}$ = 26 Hz, PPh_3), 32.7 (d, $^2J_{PP}$ = 26 Hz, PPh_3). IR (Nujol): 2277 (w, ν_{CH3CN}), 899 (s, $\nu_{W=O}$) cm^{-1}. ESI-MS (CH_2Cl_2): *m*/*z* 1066 ($[Cp^*W(O)(\mu\text{-}S)_2Ru(CH_3CN)(PPh_3)_2]^+$). Anal. Calcd for $C_{49}H_{48}F_3NO_4P_2RuS_2W$: C, 48.44; H, 3.98; N, 1.15; S, 7.92. Found: C, 48.37; H, 4.12; N, 1.29; S, 7.88.

X-ray Crystal Structure Determination. Crystal data and refinement parameters for the structurally characterized complexes are summarized in Table 5. Single crystals were coated with oil (Immersion Oil, type B: Code 1248, Cargille Laboratories, Inc.) and mounted on loops. Diffraction data were collected at −80 °C (for **4a**, **b**, **5a**, **b**, **7b**, **9**, **10**, and **11b**) or −100 °C (for **7a**) under a cold nitrogen stream on a Rigaku AFC7 equipped with a rotating anode and a MSC/ADSC Quantum 1 CCD detector (for **7a**, **b**, **10**, and **11b**), or on a Rigaku AFC5 equipped with an ADSC CCD detector (for **4a**, **b**, **5a**, **b**, and **9**) by using graphite-monochromated Mo Kα radiation (λ = 0.710690 Å). Four preliminary data frames were measured at 0.5° increments of ω, to assess the crystal quality and preliminary unit cell parameters. The intensity images were also measured at 0.5° intervals of ω. The frame data were integrated using an MSC d*TREK program package, and the data sets were corrected for absorption using a REQAB program. All calculations were performed with a TEXSAN program package. All structures were solved by direct methods. The remaining heavy atoms were found in subsequent Fourier maps, and the structures were refined by full-matrix least-squares. Anisotropic refinement was applied to all non-hydrogen atoms, except for the disordered OTf anion in **7b** were isotropically refined. The OTf anion in **7b** is disordered over two positions, with occupancy factors of 50:50. The hydrogen atoms bound to Ru in **4b**, **5b**, **7a**, and **7b** were located in the Fourier maps, and were refined isotropically, while the other hydrogen atoms were put at calculated positions. Additional data are available as Supporting Information.

Acknowledgment. This work was supported by Grant-in-Aid for Scientific Research on Priority Areas (No. 14078101, 14078211 "Reaction Control of Dynamic Complexes") from Ministry of Education, Science, Sports, and Culture, Japan.

Supporting Information Available: X-ray crystallographic information files (CIF) for the structures of **4a**, **4b**, **5a**, **5b**, **7a**, **7b**, **9**, **10**, and **11b**. This material is available free of charge via the World Wide Web at http://pubs.acs.org.

JA029941X